Struct Chem (2015) 26:749–759
DOI 10.1007/s11224-014-0534-z

ORIGINAL RESEARCH

Chemical functionalization of boron nitride nanotube via the 1,3-dipolar cycloaddition reaction of azomethine ylide: a quantum chemical study

Hossein Roohi · Mahjoubeh Jahantab · Shima Rahmdel Delcheh · Bahareh Pakdel Khoshakhlagh

Received: 9 September 2014 / Accepted: 31 October 2014 / Published online: 19 November 2014

Abstract The first principle exploration at the M05-2X/6-31+G(d,p) level was performed to investigate the chemical functionalizations of (6,0) zigzag single-walled BNNT via the 1,3-dipolar cycloaddition reaction of azomethine ylide. Two types of functionalized BNNTs (**D** and **A** complexes) were found in the reaction between 2-methoxy-*N*,*N*-dimethylethanamine (**MDE**) and BNNT. It is energetically favorable for the **MDE** functional group to interact with the B–N bonds slanted to the tube axis (in **D**-type complexes). The configuration of the lowest minimum energy corresponds to geometry **D1**, which the functional group interacts with the end of N-terminated BNNT. The results show that the functionalization of BNNT by **MDE** functional group is accompanied by a decrease in the band gap, so that this decrease in **A** complexes is greater than that in the corresponding **D** ones. Also, the results obtained by natural bond orbital analysis showed that the charge transfer occurs from nanotube to **MDE** functional group.

Keywords Functionalized BNNT · Band gap · Electronic properties · Azomethine ylide · NBO

Introduction

Since the tubular diameter and chirality have meaningful effects on the electronic properties of carbon nanotubes (CNTs), extensive studies have been performed on analogous tubular nanomaterials that their electronic properties are independent of these features [1–3]. BNNTs are the structural analog of CNTs in which alternating B and N atoms fully substitute for C atoms [4]. However, CNTs and BNNTs have similar structures, but their properties are thoroughly different. BNNTs are known as semiconductors with a wide band gap (~5.5 eV) nearly independent of tube structure [5, 6], while CNTs can show metallic or semiconductor behaviors [7–9]. In addition, BNNTs have high oxidation resistance, unique mechanical properties, high thermal conductivity, and structural stability [10, 11]. These beneficial properties make BNNTs promising materials for various potential applications.

The large band gap and chemical inertness impose great restriction on the wider applications of BNNTs. Therefore, functionalization of BNNTs either by covalent or noncovalent methods expands their potential applicability. Covalent functionalizations of BNNTs using atoms, organic molecules, and functional groups can effectively change the electronic structures [12, 13], magnetic properties [14, 15], and solubilities [16, 17] of BNNTs [18]. Thus, many experimental and theoretical studies have been reported on covalent [13, 17, 19–25] and noncovalent [18, 26–28] functionalization of BNNTs. Saikia et al. [29] utilized DFT calculation to investigate the effect of noncovalent functionalization on the structural and electronic properties of (5,5) and (10,0) BNNTs. They found that functionalization of BNNTs with isoniazid displays the presence of new impurity states within the HOMO–LUMO energy gap of pristine BNNT. The functionalization of (5,5) BNNT by $C_{10}H_7CO$, $CH_3(CH_2)_2CO$, and $CH_3(CH_2)_{16}CO$ molecules has been investigated by Zhi et al. [13]. They showed that the covalently functionalized BNNTs can be either n- or p-doped depending on the electronegativity of molecules attached. Anota et al. have investigated the properties of the chemical functionalization of (5,5)

H. Roohi (✉) · M. Jahantab · S. R. Delcheh · B. P. Khoshakhlagh
Department of Chemistry, Faculty of Science, University of Guilan, Rasht, Iran
e-mail: hroohi@guilan.ac.ir

BNNTs with levothyroxine [30], thiol, and hydroxyl groups [31] on the basis of density functional theory calculations.

In our previous works [25], we investigated the effect of CH_3CO functional group on electronic and structural properties of zigzag-type single-walled BNNTs. Functionalization of CNTs via the 1,3-dipolar cycloaddition reaction of azomethine ylides has been investigated extensively for their unique properties and many potential applications [32–35]. So far, 1,3-dipolar cycloaddition reaction of azomethine ylides with BNNT to form a functionalized BNNT has not been investigated. In this work, we have investigated structural and electronic properties of (6,0) BNNT functionalized with 2-methoxy-*N*,*N*-dimethylethanamine (**MDE**) using the M05-2X method. The changes in geometrical parameters, reaction energy, bond gaps, isodensity surfaces of highest occupied molecular orbital (HOMO) and the lowest unoccupied molecular orbital (LUMO), electrophilicity index, chemical potential, chemical hardness and softness, dipole moment, atomic charge, and the maximum amount of electronic charge are calculated. Furthermore, we have investigated atomic charge distribution in nanotubes by NBO [36] analysis.

Computational details

ONIOM approach [37, 38] has clear advantages for modeling nanoscale systems. Using this technique, it is possible to model a large system by applying a high-level quantum mechanical theory to the immediate region of interest and a lower level of theory, such as semiempirical or molecular mechanics, to the rest of the system. It can avoid the computationally prohibitive step of applying high-level theory to a system with many atoms while still yielding accurate results. In fact, ONIOM calculations have been shown to successfully model both reactions and noncovalent interactions involving nanotubes [22, 39–50]. In ONIOM approach, the full system is divided into a reactive part, which is treated at an appropriately high level of theory computationally, while the remainder of the system is included at a less-expensive lower level of theory. This ensures an appropriately high level of accuracy for the reactive part of the system while reducing the computational cost by only calculating this smaller part with the expensive method [50].

In this work, ONIOM methodology is used to study the effect of functionalization on the electronic and structural properties of BNNT. We selected a (6,0) zigzag single-walled BNNT consisting of 36 B and 36 N atoms, that the end atoms were saturated by hydrogen atoms to avoid the boundary effects. The length and diameter of optimized pure tube are computed about 11.46 and 4.92 Å, respectively. The structure of the functionalized BNNT was calculated using M05-2X functional [51] at the ONIOM(M05-2X/6-31+G(d,p):M05-2X/STO-6G) level of theory. In addition, single-point energy calculation at the M05-2X/6-31+G(d,p) level is carried out to obtain more reliable energies. All calculations have been performed using the GAUSSIAN-09 program package [52]. NBO analysis was carried out for all complexes at the M05-2X/6-31+G(d,p) level of theory.

From the optimized structures, global molecular descriptors [53–57] such as HOMO–LUMO energy gap, electronegativity (χ), chemical potential (μ), chemical hardness (η), chemical softness (S), the maximum amount of electronic charge (ΔN_{max}) that the system may accept, and electrophilicity index (ω) [58] are calculated as follows:

$$\text{Energy gap} = E_{LUMO} - E_{HOMO} \quad (1)$$

$$\mu = -\chi = -(I + A)/2 \quad (2)$$

$$\eta = (I - A)/2 \quad (3)$$

$$S = 1/2\eta \quad (4)$$

$$\Delta N_{max} = -\mu/\eta \quad (5)$$

$$\omega = \mu^2/2\eta, \quad (6)$$

where I and A are the first ionization energy and electron affinity, respectively. According to Molecular Orbital (MO) theory, the ionization potential of a molecule is simply the orbital energy of the HOMO, and the electron affinity is the orbital energy of the LUMO, with changes in sign. These are consequences of Koopmans' theorem [59, 60]. The electrophilicity index is a measure of the capacity of an electrophile to accept the maximal number of electrons in a neighboring reservoir of electron sea.

Results and discussion

Energies and geometries

The optimized geometrical parameters for monomers and functionalized BNNT (f-BNNT) are shown in Fig. 1. In whole of this work, C_B and C_N denote C atoms of **MDE** functional group connected to B and N atoms of BNNT, respectively. The circumferences of the BNNT consist of one kind of atoms, either N or B atoms; if one of the ends is formed by N atoms, the other end is formed by B atoms. Diameters of the N-terminated, B-terminated, and middle rings of pure BNNT are 5.090, 4.820, and 4.910 Å, respectively. The tube diameter at the end of N-terminated is greater than that of B-terminated. This study examines the reaction between **MDE** functional group and nanotube surface.

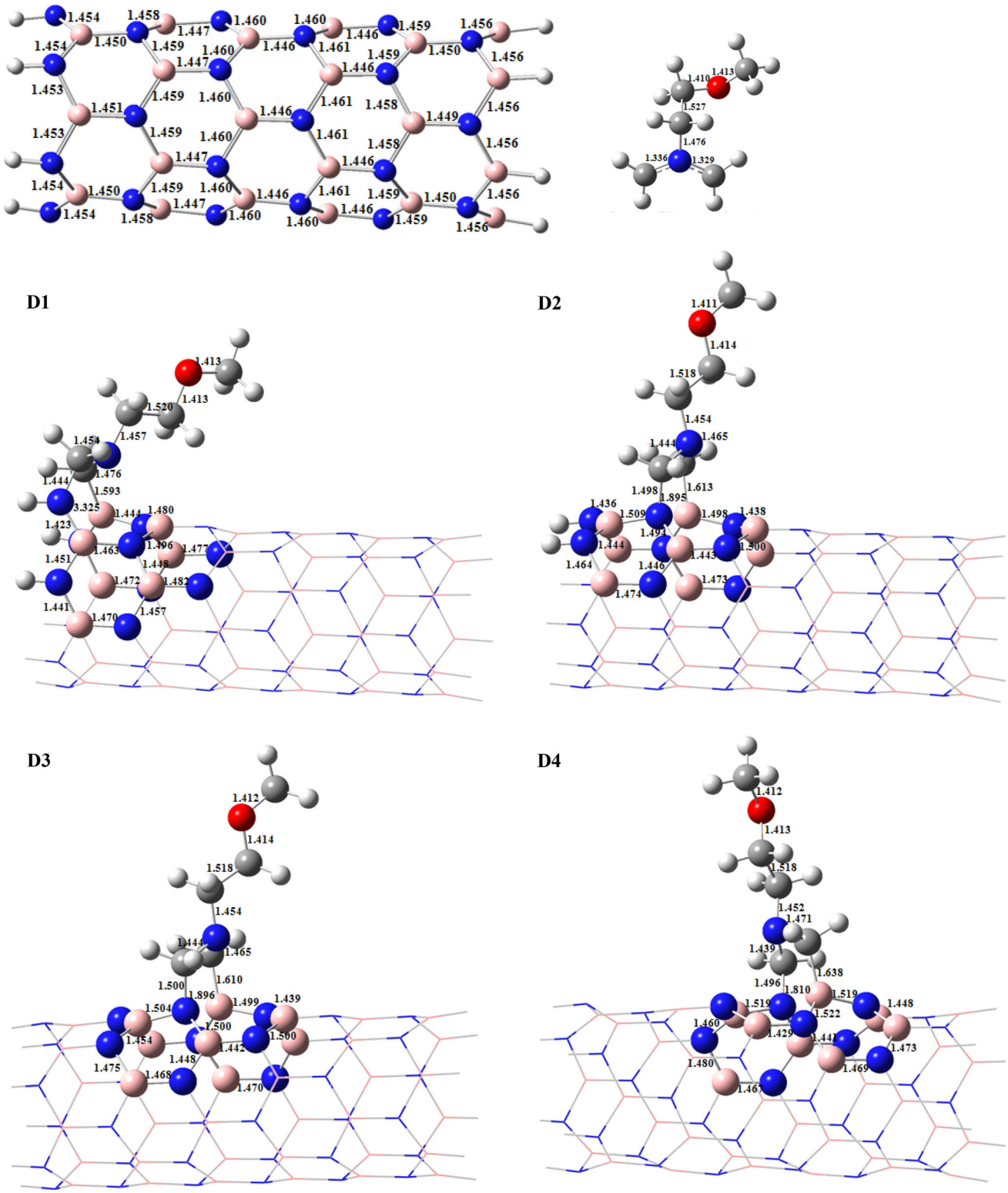

Fig. 1 Optimized structural parameters for monomers and **D1**–**A5** complexes

There are two different B–N bonds in BNNTs. The B–N bonds around the tube axis (L1) and the B–N bonds along the tube axis (L2). Since BNNTs are obtained by rolling the BN graphene-like sheet, the slanted B–N bonds have a larger local curvature in zigzag BNNTs and are more reactive than the B–N bonds parallel to the tube axis. As

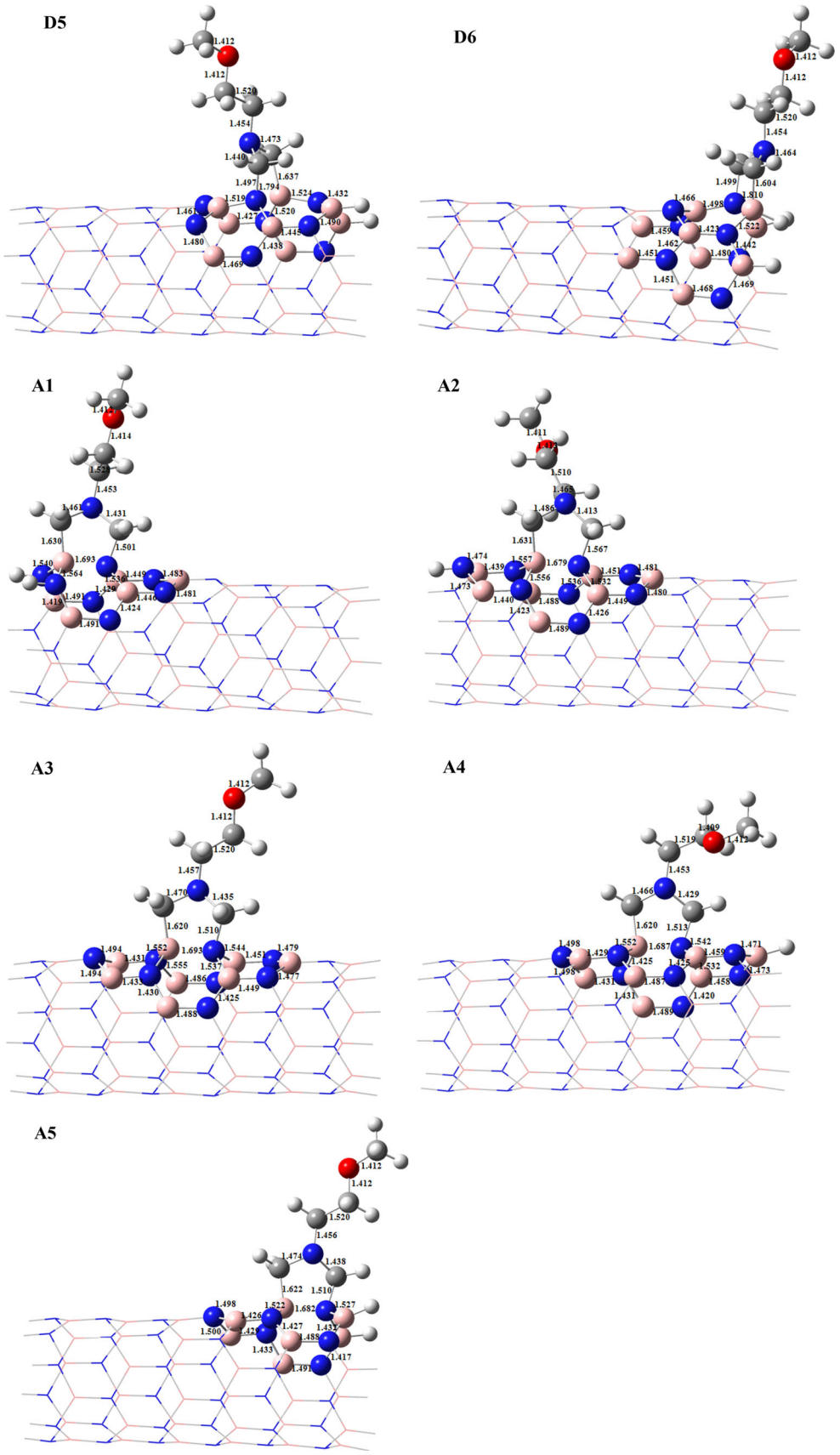

Fig. 1 continued

shown in Fig. 1, due to the greater curvature, the L1 bond lengths in the pristine NT are longer than L2 ones, indicating that the slanted L1 bonds are more reactive than the L2 bonds paralleled to the tube axis.

All L1 and L2 bonds on the sidewall of BNNT were considered for attachment of an individual **MDE** functional group. We found the eleven minima energy structures on the potential energy surface (Fig. 1). For axial (**A**) and diagonal (**D**) structures, **MDE** is bonded to the L2 and L1 bonds of BNNT, respectively.

Because of the iconicity of B–N bonds, results show that in the addition of **MDE** to the B–N bonds of zigzag BNNTs, the formation of open structures is preferable for mentioned tube. As can be seen, diagonal B–N bonds increase from an average value of 1.458 Å in pristine BNNT to 3.325, 1.895, 1.896, 1.810, 1.794, and 1.810 Å, in **D1**-**D6** complexes, respectively. In configuration **D1**, the **MDE** functional group interacting with the end of N-terminated BNNT leads to the opening B–N bond. Thus, the longest diagonal B–N bond attached to **MDE** is observed in **D1** complex. The increase in diagonal B–N bonds of B-terminated BNNT is shorter than that in the middle bonds. For the **D** structures, the newly B–C and N–C chemical bonds formed between **MDE** and BNNT make a nine-membered ring, thus inducing a local structural deformation in BNNT.

The optimized geometries of the **D** group of f-BNNT exhibit the B–C and N–C bond lengths of 1.593 and 1.423 Å in **D1**, 1.613 and 1.498 Å in **D2**, 1.610 and 1.500 Å in **D3**, 1.638 and 1.496 Å in **D4**, 1.637 and 1.497 Å in **D5**, and 1.604 and 1.499 Å in **D6**, respectively. These results reveal that the N–C bonds are shorter than B–C bonds. The average values of B–C and N–C bond lengths are 1.508, 1.556, 1.555, 1.567, 1.567, and 1.552 Å, respectively. These results indicate that the reactions between **MDE** and B–N bonds at the end of N-terminated and B-terminated BNNT are stronger than other bonds. Thus, these sites in BNNT are favored for functionalization by **MDE**.

The length of N–C bond in the **A1**–**A5** complexes is 1.510, 1.567, 1.510, 1.513, and 1.501 Å and that of B–C bond is 1.631, 1.635, 1.620, 1.620, and 1.622 Å, respectively. As can be seen, similar to **D** group of complexes, the B–C bonds in **A** group of complexes are longer than N–C bonds. The average value of B–C and N–C bond lengths are 1.571, 1.601, 1.565, 1.567, and 1.562 Å, respectively, showing that the bonds formed in **A5** complex are stronger than those in **A1**–**A4** ones. Thus, L2 bond in the end of B-terminated BNNT is favored for reaction with **MDE** functional group. In addition, comparison of the bonds formed between **MDE** and BNNT in **A** and **D** complexes shows that the bonds in **D** complexes are stronger than those in **A** ones.

As shown in Fig. 1, the axial (L2) B–N bond lengths increase from an average value of 1.448 Å in pristine BNNT to 1.693, 1.679, 1.693, 1.687, and 1.682 Å in the **A1**–**A5** complexes, respectively. Comparison of B–N bonds in two types of complexes shows that the change in B–N bond length upon functionalization of BNNT in **D** complexes is bigger than that in the **A** ones.

The complex formation also leads to structural changes in **MDE** molecule. The C atoms of the **MDE** bonded to N and B atoms of NT are symbolized as C_N–N and C_B–N, respectively. For the free **MDE** functional group, the optimized C_N–N and C_B–N bond lengths are 1.336 and 1.329 Å, respectively. The C_B–N (C_N–N) bond lengths of **D1**-**D6** complexes are 1.476 (1.454), 1.465 (1.444), 1.465 (1.444), 1.471 (1.438), 1.473 (1.440), and 1.464 (1.442) Å,

Table 1 Total energy, relative energy, reaction energies (RE), and dipole moment for BNNT-**MDE** system at M05-2X/6-31+G(d,p) level of theory

Configuration	Total energy, Hartree	ΔE, kcal mol^{-1}	RE, kcal mol^{-1}	Dipole moment, Debye
Diagonal structures				
D1	−3203.863130	0.0	−37.0	8.61
D2	−3203.840147	14.4	−22.1	8.30
D3	−3203.837258	16.2	−20.3	7.92
D4	−3203.837754	15.9	−20.7	8.11
D5	−3203.837431	16.1	−20.5	8.26
D6	−3203.845480	11.1	−25.7	7.47
Axial structures				
A1	−3203.832203	19.4	−17.2	3.90
A2	−3203.838914	15.2	−21.4	3.50
A3	−3203.836977	16.4	−20.0	1.68
A4	−3203.835263	17.5	−19.1	3.81
A5	−3203.843909	12.1	−24.5	2.01

respectively, showing that both the C_N–N and C_B–N bond lengths increase upon complex formation, so that this increase in **D1** complex is greater than that in the other ones. For **A1**–**A5** complexes, the optimized C_B–N and C_N–N bond lengths are (1.467 and 1.431), (1.486 and 1.414), (1.471 and 1.435), (1.466 and 1.429), and (1.471 and 1.438), respectively.

Total energy, relative energy, reaction energy (RE), and dipole moment of the **D** and **A** compounds are summarized in Table 1. Relative energy of f-BNNTs in **D1**–**D6** is 0.0, 14.4, 16.2, 15.9, 16.1, and 11.1 kcal/mol and that of **A1**–**A5** is 19.4, 15.2, 16.4, 17.5, and 12.1 kcal/mol, respectively. Thus, **D1** in the **D** group complexes and **A5** in the **A** ones are more stable than other complexes in each group of compounds, in good agreement with the predicted structural parameters involved in the reaction.

The calculated reaction energies for **A** and **D** complexes at M05-2X/6-31+G(d,p) level of theory are presented in Table 1. The RE is defined as $RE = E_{complex} - (E_{BNNT} + E_{MDE})$, where $E_{complex}$ is the total energy of the BNNT-**MDE** system. As can be seen in Table 1, RE values for **D1**, **D2**, **D3**, **D4**, **D5,** and **D6** complexes are −37.0, −22.1, −20.3, −20.7, −20.5, and −25.7 kcal mol^{-1} and for **A1**, **A2**, **A3**, **A4**, and **A5** complexes are −17.2, −21.4, −20.0, −19.1, and −24.5 kcal mol^{-1}, respectively. The negative RE means exothermic addition reaction on BNNT sidewalls. Comparison of REs reveals that the stability of complexes decreases in the order of **D1** > **D6** > **D2** > **D4** > **D5** > **D3** for **D** complexes and **A5** > **A2** > **A3** > **A4** > **A1** for **A** complexes. It is evident from the RE values that the **D** complexes are more stable than **A** complexes. According to these results, it is energetically favorable for the **MDE** functional group to interact with the slanted B–N bonds at the end of the N-terminated (**D1**), due to the rather large local curvature of this kind of B–N bonds, and B-terminated (**D6**) BNNT and axial B–N bonds at the end of the B-terminated (**A5**) BNNT. The reaction energies obtained for attachment of the **MDE** to BNNT are comparable with that of reported [33] for attachment to (5,5) CNT at PBE/6-31G* level (20.3 kcal mol^{-1}).

Frontier molecular orbitals

The influences of functional group on electron density distributions of HOMOs and LUMOs have also been investigated. Figure 2 presents the isodensity surfaces of the HOMOs and LUMOs of pristine and functionalized BNNT. It can be seen that the HOMO in **MDE** is quite localized on the CH_2 groups, indicating a tendency of molecule to react through the CH_2 groups. The HOMO in pristine BNNT is quite localized on the N atoms at the end of N-terminated, whereas LUMO is distributed on axial B–N bonds and mainly on the end of B-terminated. For the f-BNNTs, the HOMO states are basically localized on the **MDE** functional group and in the vicinity of the covalently attached functional group, whereas electron density of LUMO is distributed on the B–N pairs along the tube axis and mainly on the end of B–terminated. The analysis of the electron density distributions of HOMOs and LUMOs reveal that the upon electronic excitation from HOMO to LUMO, electron density on the **MDE** decreases.

Fig. 2 The isodensity surface of HOMO and LUMO for **MDE**, pristine BNNT, and **D1**–**A5** complexes at the isovalue of 0.02. N and B atoms are represented by *blue* and *pink spheres*

Global reactivity descriptors

To better understand the effect of functional group on the electronic properties of BNNT, the electronic structures of pristine and functionalized BNNT were investigated. The frontier molecular orbitals, HOMO–LUMO energy gap, μ, η, S, ω, and ΔN_{max} are tabulated in Table 2.

The energy gap between HOMO and LUMO usually defines the lowest electronic energy absorption band [55]. A high HOMO–LUMO energy gap indicates greater stability and low reactivity of the chemical system. Hard molecules have a large energy gap, and soft molecules have a small energy gap. A soft molecule with a small gap will be more polarizable than hard molecules.

As can be seen in Table 2, the bond gap of pure nanotube is calculated as 7.17 eV. After attachment of **MDE**, the bond gap between HOMO and LUMO decreases, implying an increase in reactivity of the f-BNNT systems. Decrease in bond gaps upon complex formation of **A** complexes is greater than those of the corresponding **D** complexes. Although stability of **D** complexes is greater than that of the **A** ones, the conductivity of **A** complexes is predicted to be greater than that of the **D** ones. The conductivity of complexes increases in the order of **A2** > **A1** > **A3** ~ **A4** > **A5** > **D1** > **D2** > **D6** > **D4** > **D5** > **D3**. Comparison of values in Table 2 indicates that chemical potential, hardness, and electrophilicity index (with the exception of **A3**) decrease and the chemical softness increases upon functionalization. On the other hand, functionalization of BNNT by **MDE** functional group is accompanied with the increase of ΔN_{max} in **A** complexes and decrease in **D** ones.

The DOS (shown in Fig. 3) of pure and f-BNNTs was plotted to illustrate how the functional group affects the electronic structure of the BNNTs. As can be seen in this figure, the DOS of BNNT/**MDE** complexes is significantly changed when the **MDE** is localized on the BNNT surface. Figure 2 also shows that the presence of **MDE** on the BNNTs decreases the band gap of the pure BNNT and increases its electrical conductance.

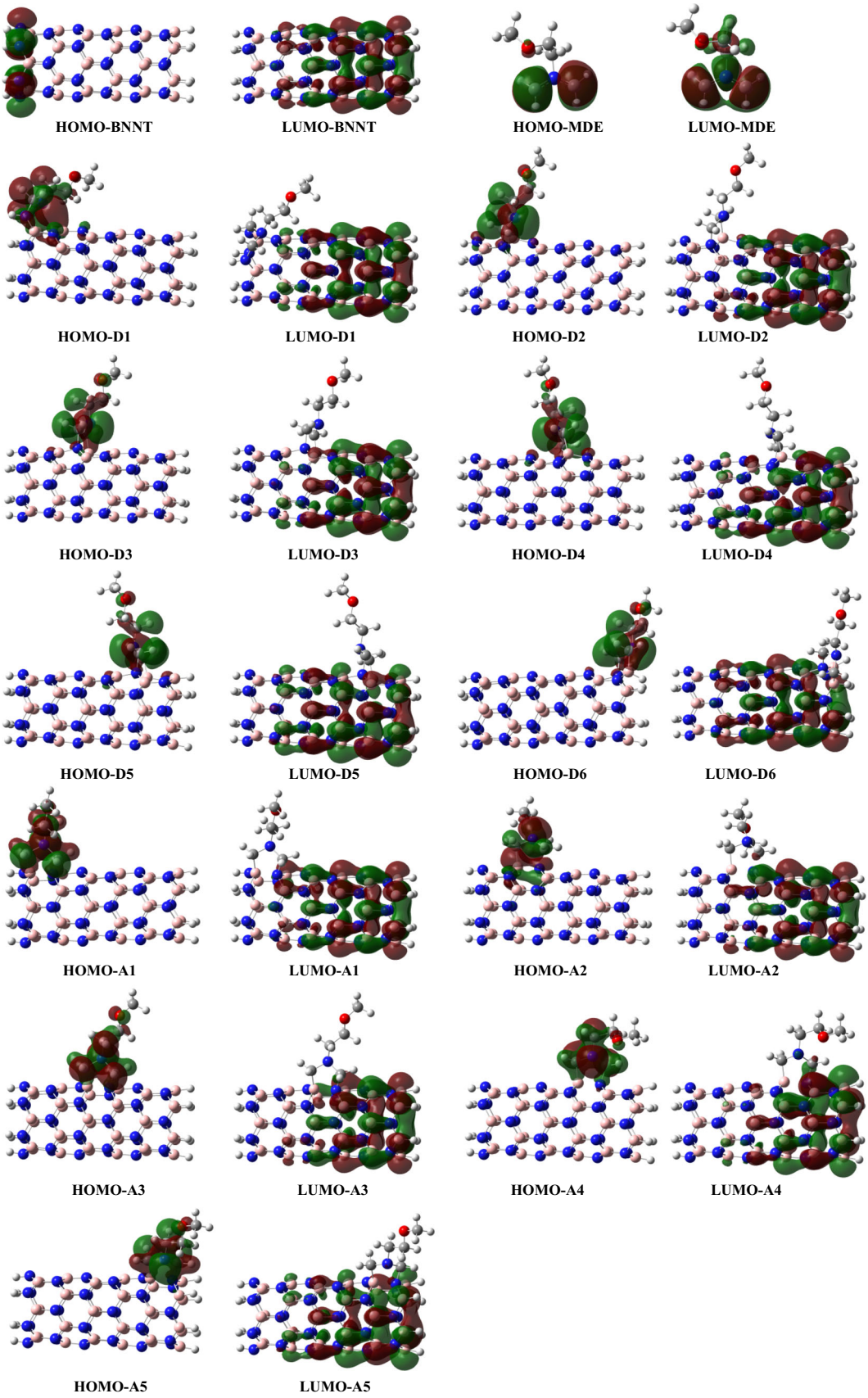
HOMO-BNNT
LUMO-BNNT
HOMO-MDE
LUMO-MDE
HOMO-D1
LUMO-D1
HOMO-D2
LUMO-D2
HOMO-D3
LUMO-D3
HOMO-D4
LUMO-D4
HOMO-D5
LUMO-D5
HOMO-D6
LUMO-D6
HOMO-A1
LUMO-A1
HOMO-A2
LUMO-A2
HOMO-A3
LUMO-A3
HOMO-A4
LUMO-A4
HOMO-A5
LUMO-A5

Table 2 HOMO energy (E_{HOMO}), LUMO energy (E_{LUMO}), HOMO–LUMO energy gap ($E_{L–H}$), electronic chemical potential (μ), chemical hardness (η), chemical softness (S), electrophilicity index (ω), and the maximum amount of electronic charge (ΔN_{max}) for **MDE**, pristine BNNT, and functionalized BNNT

	E_{HOMO}, eV	E_{LUMO}, eV	$E_{L–H}$, eV	μ, eV	η, eV	S, eV^{-1}	ω, eV	ΔN_{max}, a.u.
BNNT	−8.46	−1.29	7.17	4.88	3.58	0.14	3.32	−1.36
MDE	−5.45	0.54	4.90	3.00	2.45	0.20	1.83	−1.22
D1	−7.83	−1.02	6.82	4.43	3.41	0.15	2.87	−1.30
D2	−7.90	−0.99	6.90	4.45	3.45	0.14	2.86	−1.29
D3	−7.99	−0.95	7.04	4.47	3.52	0.14	2.84	−1.27
D4	−7.91	−0.98	6.93	4.44	3.46	0.14	2.85	−1.28
D5	−7.97	−0.99	6.98	4.48	3.49	0.14	2.88	−1.28
D6	−7.94	−1.02	6.93	4.48	3.46	0.14	2.90	−1.29
A1	−7.57	−1.27	6.30	4.42	3.15	0.16	3.10	−1.40
A2	−7.51	−1.32	6.18	4.41	3.09	0.16	3.15	−1.43
A3	−7.99	−1.40	6.58	4.70	3.29	0.15	3.35	−1.43
A4	−7.95	−1.37	6.58	4.66	3.29	0.15	3.30	−1.42
A5	−8.06	−1.28	6.81	4.68	3.41	0.15	3.22	−1.38

NBO analysis

Among theoretical methods, NBO analysis is a unique approach to the evaluation of the atomic charges and charge transfer energies. The NBO analysis reveals interesting details on the electron density transfer in donor → acceptor interactions [36]. The results of NBO analysis at the M05-2X/6-31+G(d,p) level of theory are given in Table 3. It is clear that the charges of N and B atoms in these structures are negative and positive, respectively. According to NBO analysis, the strongest effect of the functional group on the net charges takes place on B and N atoms connected to the functional group. It can be seen from Table 3 that the positive charge of B atoms and negative charge of N atoms connected to **MDE** functional group in all complexes decrease upon complexation. In all complexes, the negative charge of C_B atom of f-BNNT increases upon complex formation and that of C_N atom of f-BNNT decreases. The negative charges of C_B atoms are larger than those of the corresponding C_N atoms. Also the negative charge of N atom of **MDE** functional group connected to C atoms increases upon functionalization.

Table 3 also shows that the charge transfer (CT) occurs from nanotube to **MDE** group (with the exception of **A2**). In the **A2** complex, the charge is transferred from **MDE** group to the nanotube. The CT values for **D1**–**D6** complexes are 0.0502, 0.0277, 0.0172, 0.0150, 0.0006, and 0.0189 au and in **A1**, **A2**, **A3**, **A4**, and **A5** complexes are 0.0348, 0.0429, 0.0193, 0.0115, and 0.0137, respectively. The amount of charge transfer has been defined as the sum of electronic charge of atoms in **MDE** functional group.

Conclusions

In this paper, we have studied the structural and electronic properties of the covalent functionalization of (6,0) BNNT surface with **MDE** functional group based on density functional calculations. There are two different B–N bonds in BNNTs. The B–N bonds around the tube axis are designed as L1 and the B–N bonds along the tube axis are labeled as L2. All B–N bonds on the sidewall of BNNT were considered for adsorption of an individual **MDE** group. For axial (**A**) and diagonal (**D**) structures, **MDE** is located on the L2 and L1 bonds of BNNT, respectively. Due to the greater curvature, the L1 bonds are more reactive than the B–N bonds parallel to the tube axis. The results show that the reaction of **MDE** with (6,0) BNNT is exothermic. It is evident from reaction energies that the **D** complexes are more stable than the **A** ones. The configuration of the lowest minimum energy corresponds to geometry **D1**, in which the functional group interacts with N-terminated of the BNNT.

Functionalization of BNNT by **MDE** functional group is accompanied by a decrease in the band gap of the pure BNNT and an increase in the electrical conductance. Decrease in band gap of nanotubes for **A** complexes is greater than that for corresponding **D** complexes. Also, the chemical potential, hardness, and electrophilicity index decrease and the chemical softness increases upon functionalization. In addition, we have considered the

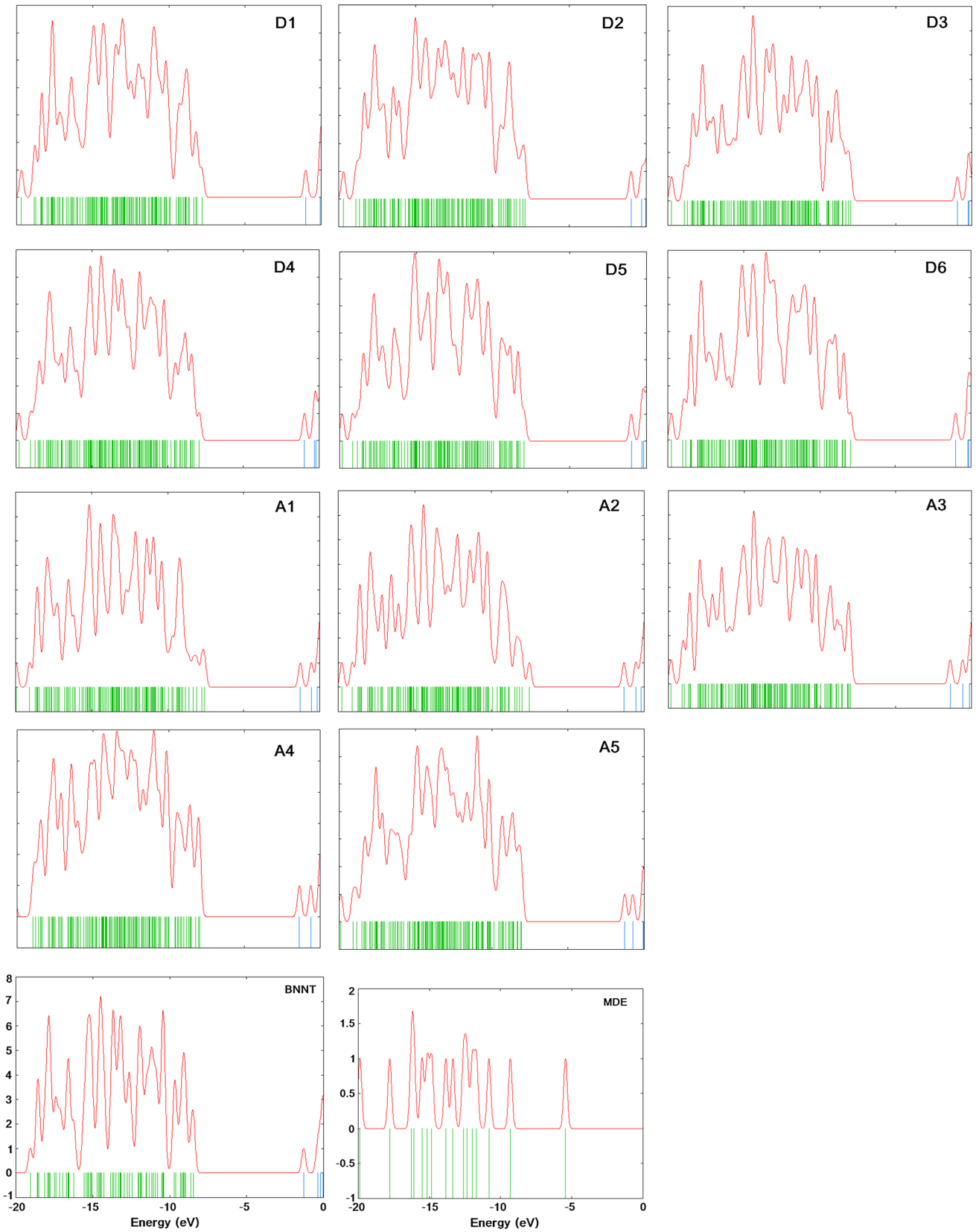

Fig. 3 Density of states (DOS) for **MDE**, pristine BNNT, and **D1**–**A5** complexes

Table 3 NBO results calculated at the M05-2X/6-31+G(d,p) level of theory

	D1	D2	D3	D4	D5	D6
Natural charge						
N^a	−0.955 (−1.167)	−1.046 (−1.225)	−1.051 (−1.222)	−1.050 (−1.222)	−1.057 (−1.223)	−1.052 (−1.220)
B^a	1.053 (1.153)	1.050 (1.216)	1.048 (1.220)	1.024 (1.222)	1.008 (1.219)	0.575 (0.854)
C_B^a	−0.617 (−0.411)	−0.612	−0.611	−0.601	−0.593	−0.586
C_N^a	−0.065 (−0.459)	−0.046	−0.046	−0.052	−0.045	−0.049
N	−0.561 (−0.286)	−0.557	−0.555	−0.559	−0.562	−0.555
CT	−0.0502	−0.0277	−0.0172	−0.0150	−0.0006	−0.0189
	A1	**A2**	**A3**	**A4**		**A5**
Natural charge						
N^a	−1.023 (−1.225)	−1.061 (−1.222)	−1.024 (−1.222)	−1.029 (−1.223)		−1.037 (−1.220)
B^a	0.963 (1.153)	0.980 (1.216)	1.008 (1.220)	1.007 (1.222)		0.995 (1.219)
C_B^a	−0.587	−0.598	−0.597	−0.594		−0.596
C_N^a	−0.048	−0.056	−0.048	−0.052		−0.057
N	−0.549	−0.536	−0.550	−0.542		−0.549
CT	−0.0348	0.0429	−0.0193	−0.0115		−0.0137

The atomic natural charges for monomers are given in parentheses. The charge transfer (CT) values are the sum of the atomic charges corresponding to the **MDE** fragment in tubes

[a] Atoms involved in interaction

isodensity surfaces of the HOMOs and LUMOs for pure and f-BNNTs. Also, the results obtained by NBO analysis showed that the charge transfer occurs from nanotube to **MDE** group (with the exception of **A2**).

References

1. Saito R, Dresselhaus G, Dresselhaus MS (1998) Physical properties of carbon nanotubes, vol 4. World Scientific, Singapore
2. White CT, Mintmire JW (2005) Fundamental properties of single-wall carbon nanotubes. J Phys Chem B 109(1):52–65
3. Zhang M, Su Z-M, Yan L-K, Qiu Y-Q, Chen G-H, Wang R-S (2005) Theoretical interpretation of different nanotube morphologies among Group III (B, Al, Ga) nitrides. Chem Phys Lett 408(1):145–149
4. Chopra NG, Luyken R, Cherrey K, Crespi VH, Cohen ML, Louie SG, Zettl A (1995) Boron nitride nanotubes. Science 269(5226):966–967
5. Rubio A, Corkill JL, Cohen ML (1994) Theory of graphitic boron nitride nanotubes. Phys Rev B 49(7):5081
6. Blase X, Rubio A, Louie S, Cohen M (1994) Stability and band gap constancy of boron nitride nanotubes. EPL (Europhys Lett) 28(5):335–340
7. Hamada N, Sawada S-I, Oshiyama A (1992) New one-dimensional conductors: graphitic microtubules. Phys Rev Lett 68(10):1579–1581
8. Saito R, Fujita M, Dresselhaus G, Dresselhausu M (1992) Electronic structure of chiral graphene tubules. Appl Phys Lett 60(18):2204–2206
9. Esrafili MD, Behzadi H (2013) A DFT study on carbon-doping at different sites of (8, 0) boron nitride nanotube. Struct Chem 24(2):573–581
10. Tang C, Bando Y (2003) Effect of BN coatings on oxidation resistance and field emission of SiC nanowires. Appl Phys Lett 83(4):659–661
11. Xiao Y, Yan X, Xiang J, Mao Y, Zhang Y, Cao J, Ding J (2004) Specific heat of single-walled boron nitride nanotubes. Appl Phys Lett 84(23):4626–4628
12. Tang C, Bando Y, Huang Y, Yue S, Gu C, Xu F, Golberg D (2005) Fluorination and electrical conductivity of BN nanotubes. J Am Chem Soc 127(18):6552–6553
13. Zhi C, Bando Y, Tang C, Golberg D (2006) Engineering of electronic structure of boron-nitride nanotubes by covalent functionalization. Phys Rev B 74(15):153413
14. Gou G, Pan B, Shi L (2008) Interaction of iron atoms with pristine and defective (8, 0) boron nitride nanotubes. J Phys Chem C 112(35):13571–13578
15. Chen Z-G, Zou J, Li F, Liu G, Tang D-M, Li D, Liu C, Ma X, Cheng H-M, Lu GQ (2007) Growth of magnetic yard-glass shaped boron nitride nanotubes with periodic iron nanoparticles. Adv Funct Mater 17(16):3371–3376
16. Zhi C, Bando Y, Tang C, Honda S, Sato K, Kuwahara H, Golberg D (2005) Covalent functionalization: towards soluble multiwalled boron nitride nanotubes. Angew Chem Int Ed 44(48):7932–7935
17. Wu X, An W, Zeng XC (2006) Chemical functionalization of boron-nitride nanotubes with NH_3 and amino functional groups. J Am Chem Soc 128(36):12001–12006
18. Gou G, Pan B, Shi L (2010) Noncovalent functionalization of BN nanotubes with perylene derivative molecules: an ab initio study. ACS Nano 4(3):1313–1320
19. Zhou Z, Zhao J, Chen Z, Schleyer PVR (2006) Atomic and electronic structures of fluorinated BN nanotubes: computational study. J Phys Chem B 110(51):25678–25685
20. Zhi C, Bando Y, Tang C, Golberg D (2006) SnO_2 nanoparticle-functionalized boron nitride nanotubes. J Phys Chem B 110(17):8548–8550
21. Li Y, Zhou Z, Zhao J (2008) Functionalization of BN nanotubes with dichlorocarbenes. Nanotechnology 19(1):015202

22. Ahmadi A, Beheshtian J, Hadipour NL (2011) Chemisorption of NH_3 at the open ends of boron nitride nanotubes: a DFT study. Struct Chem 22(1):183–188
23. J-x Zhao, Y-h Ding (2009) Theoretical studies of chemical functionalization of the (8, 0) boron nitride nanotube with various metalloporphyrin MP (M = Fe Co, Ni, Cu, and Zn) complexes. Mater Chem Phys 116(1):21–27
24. Z-y Yang, Li Y-F, Zhou Z (2009) Functionalization of BN nanotubes with free radicals: electroaffinity-independent configuration and band structure engineering. Front Phys China 4:378–382
25. Roohi H, Nowroozi A-R, Ebrahimi A, Makiabadi B (2010) Effect of CH_3CO functional group on the molecular and electronic properties of BN43zz nanotube: a computational chemistry study. J Mol Struct (Thoechem) 952(1):36–45
26. Wang W, Bando Y, Zhi C, Fu W, Wang E, Golberg D (2008) Aqueous noncovalent functionalization and controlled near-surface carbon doping of multiwalled boron nitride nanotubes. J Am Chem Soc 130(26):8144–8145
27. J-x Zhao, Y-h Ding (2010) Theoretical study of noncovalent functionalization of BN nanotubes by various aromatic molecules. Diam Relat Mater 19(7):1073–1077
28. Velayudham S, Lee CH, Xie M, Blair D, Bauman N, Yap YK, Green SA, Liu H (2010) Noncovalent functionalization of boron nitride nanotubes with poly (p-phenylene-ethynylene) and polythiophene. ACS Appl Mater Interfaces 2(1):104–110
29. Saikia N, Pati SK, Deka RC (2012) First principles calculation on the structure and electronic properties of BNNTs functionalized with isoniazid drug molecule. Appl Nanosci 2(3):389–400
30. Anota EC, Cocoletzi GH, Ramírez JS (2013) Armchair BN nanotubes—levothyroxine interactions: a molecular study. J Mol Model 19(11):4991–4996
31. Anota EC, Cocoletzi GH (2013) First-principles simulations of the chemical functionalization of (5,5) boron nitride nanotubes. J Mol Model 19(6):2335–2341
32. Georgakilas V, Voulgaris D, Vazquez E, Prato M, Guldi DM, Kukovecz A, Kuzmany H (2002) Purification of HiPCO carbon nanotubes via organic functionalization. J Am Chem Soc 124:14318–14319
33. Denis PA (2011) Improving the chemical reactivity of single-wall carbon nanotubes with lithium doping. J Phys Chem C 115:20282–20288
34. Georgakilas V, Kordatos K, Prato M, Guldi DM, Holzinger M, Hirsch A (2002) Organic functionalization of carbon nanotubes. J Am Chem Soc 124:760–761
35. Georgakilas V, Tagmatarchis N, Pantarotto D, Bianco A, Briand J-P, Prato M (2002) Amino acid functionalization of water soluble carbon nanotubes. Chem Commun 3050–3051.
36. Reed AE, Curtiss LA, Weinhold F (1988) Intermolecular interactions from a natural bond orbital donor-acceptor viewpoint. Chem Rev 88(6):899–926
37. Svensson M, Humbel S, Froese R, Matsubara T, Sieber S, Morokuma K (1996) ONIOM: a multilayered integrated MO + MM method for geometry optimizations and single point energy predictions a test for Diels–Alder reactions and $Pt(P(t\text{-}Bu)_3)_2 + H_2$ oxidative addition. J Phys Chem 100:19357–19363
38. Vreven T, Byun KS, Komáromi I, Dapprich S, Montgomery JA Jr, Morokuma K, Frisch MJ (2006) Combining quantum mechanics methods with molecular mechanics methods in ONIOM. J Chem Theory Comput 2:815–826
39. Basiuk VA (2003) ONIOM studies of chemical reactions on carbon nanotube tips: effects of the lower theoretical level and mutual orientation of the reactants. J Phys Chem B 107:8890–8897
40. Kar T, Akdim B, Duan X, Pachter R (2004) A theoretical study of functionalized single-wall carbon nanotubes: ONIOM calculations. Chem Phys Lett 392:176–180
41. Lu X, Tian F, Zhang Q (2003) The [2+1] cycloadditions of dichlorocarbene, silylene, germylene, and oxycarbonylnitrene onto the sidewall of armchair (5,5) single-wall carbon nanotube. J Phys Chem B 107:8388–8391
42. Liu LV, Tian WQ, Wang YA (2006) Ozonization at the vacancy defect site of the single-walled carbon nanotube. J Phys Chem B 110:13037–13044
43. Tetasang S, Keawwangchai S, Wanno B, Ruangpornvisuti V (2012) Quantum chemical investigation on structures of pyrrolic amides functionalized (5,5) single-walled carbon nanotube and their binding with halide ions. Struct Chem 23:7–15
44. Luoxin W, Changhai Y, Hantao Z, Houlei G, Jie X, Weilin X (2011) Initial reactions of methyl-nitramine confined inside armchair (5,5) single-walled carbon nanotube. J Mol Model 17:2751–2758
45. Lu X, Tian F, Wang N, Zhang Q (2002) The viability of the Diels–Alder (DA) cycloaddition of conjugated dienes onto the sidewalls of single-wall carbon nanotubes is assessed by means of a two-layered ONIOM(B3LYP/6-31G*:AM1) approach. Org Lett 4(24):4313–4315
46. Basiuk VA (2002) Reactivity of carboxylic groups on armchair and zigzag carbon nanotube tips: a theoretical study of esterification with methanol. Nano Lett 2(8):835–839
47. Xu Y-J, Li J-Q (2005) The interaction of N_2 with active sites of a single-wall carbon nanotube. Chem Phys Lett 412:439–443
48. Schatz GC (2007) Using theory and computation to model nanoscale properties. Proc Natl Acad Sci USA 104(17):6885–6892
49. Torrent M, Vreven T, Musaev DG, Morokuma K, Farkas Ö, Schlegel HB (2002) Effects of the protein environment on the structure and energetics of active sites of metalloenzymes. ONIOM study of methane monooxygenase and ribonucleotide reductase. J Am Chem Soc 124(2):192–193
50. Vreven T, Thompson LM, Larkin SM, Kirker I, Bearpark MJ (2012) Deconstructing the ONIOM Hessian: investigating method combinations for transition structures. J Chem Theory Comput 8:4907–4914
51. Zhao Y, Schultz NE, Truhlar DG (2006) Design of density functionals by combining the method of constraint satisfaction with parametrization for thermochemistry, thermochemical kinetics, and noncovalent interactions. J Chem Theory Comput 2(2):364–382
52. Frisch M, Trucks G, Schlegel HB, Scuseria G, Robb M, Cheeseman J, Scalmani G, Barone V, Mennucci B, Petersson G (2009) Gaussian 09, Revision A. 02, Gaussian. Inc, Wallingford, CT 2009.
53. Chattaraj PK, Sarkar U, Roy DR (2006) Electrophilicity index. Chem Rev 106(6):2065–2091
54. Pearson RG (1989) Absolute electronegativity and hardness: applications to organic chemistry. J Org Chem 54(6):1423–1430
55. Parr RG, Zhou Z (1993) Absolute hardness: unifying concept for identifying shells and subshells in nuclei, atoms, molecules, and metallic clusters. Acc Chem Res 26(5):256–258
56. Parr RG, Donnelly RA, Levy M, Palke WE (1978) Electronegativity: the density functional viewpoint. J Chem Phys 68(8):3801–3807
57. Parr RG, Pearson RG (1983) Absolute hardness: companion parameter to absolute electronegativity. J Am Chem Soc 105(26):7512–7516
58. Parr RG, Szentpály LV, Liu S (1999) Electrophilicity index. J Am Chem Soc 121(9):1922–1924
59. Pearson RG (1987) Recent advances in the concept of hard and soft acids and bases. J Chem Educ 64(7):561–567
60. Koopmans T (1934) Über die Zuordnung von Wellenfunktionen und Eigenwerten zu den einzelnen Elektronen eines Atoms. Physica 1(1):104–113